



# Magnetic and Electrical Transport Properties of Double Perovskite Sr<sub>2</sub>FeMoO<sub>6</sub> Prepared by Sol-Gel Method

YONG-QING ZHAI\*, JING QIAO and ZHANG ZHANG

College of Chemistry and Environmental Science, Hebei University  
Baoding, 071002, People's Republic of China  
*zhaiyongqinghbu@163.com*

Received 2 April 2011; Accepted 7 June 2011

**Abstract:** With activated carbon for reducing agent, the sol-gel method was used to prepare the giant magnetoresistance materials Sr<sub>2</sub>FeMoO<sub>6</sub>, which is the double Perovskite oxide. The structure, morphology, magnetic and electrical transport properties were investigated respectively by x-ray diffraction, scanning electron microscopy and vibrating sample magnetometer. The as-synthesized sample is Sr<sub>2</sub>FeMoO<sub>6</sub> with tetragonal crystal structure and I4/mmm space group and unit cell parameter is  $a = 5.580\text{\AA}$ ,  $c = 7.882\text{\AA}$ . The primary particles are spherical in shape and the grain size is below 100 nm. The curie temperature is above room temperature and the saturation magnetization is  $13.321\text{ A}\cdot\text{m}^2/\text{kg}$  under 1.0 T at room temperature. The sample exhibit typical semiconductor behavior and the conductive mechanism can be described by small polaron variable range hopping model. The room temperature magnetoresistance of the sample under 1.0 T field is up to -10.02%. Moreover, it is found the dosage of citric acid and the amount of reducing agent has great effect on the phase structure and magnetic properties of the samples.

**Keywords:** Sol-Gel method, Double-perovskite, Sr<sub>2</sub>FeMoO<sub>6</sub>, Magnetoresistance, Conductive mechanism

## Introduction

Ten years after the discovery of giant magnetoresistance (GMR), the observation at room temperature of a large magnetoresistance in magnetic tunnel junctions gave rise to an increase of the interest for these systems mainly due to their potential applications such as recording media, field sensors or heads for hard drives<sup>1,2</sup>.

The physical properties of Perovskite La<sub>1-x</sub>A<sub>x</sub>MnO<sub>3</sub> (A = Ca, Ba, Sr) have been widely studied in the past. The discovery of giant magnetoresistance effects has renewed the interest in such compounds<sup>3-6</sup>. Double perovskites were studied in the late 1950s, but the double Perovskite Sr<sub>2</sub>FeMoO<sub>6</sub> has been brought recently into the center of scientific interest because

of its considerable magnetoresistance observed already in the relatively low magnetic fields even at and above room temperature<sup>7-9</sup>, which offers potential applications in spintronic devices and is of fundamental interest in condensed matter physics.

The compounds  $\text{Sr}_2\text{FeMoO}_6$  reported previously is prepared by the traditional solid state reaction<sup>10</sup>, which is carried out at a higher sintering temperature and therefore only the polycrystalline materials with a large grain size are produced. Band calculations indicated  $\text{Sr}_2\text{FeMoO}_6$  had a half-metallic electronic state and its magnetoresistance (MR) has been assumed to be dominated by spin-polarized tunneling through insulating grain boundaries<sup>7</sup>. Its smaller grain size leads to larger MR effect at low applied field, so large grains are not beneficial to enhance the low field MR<sup>11</sup>. It is well known that Sol-gel method is one of preparation methods for nano-sized materials and homogeneous components can be obtained in relatively low temperature.

In this paper, sol-gel method was used to synthesis  $\text{Sr}_2\text{FeMoO}_6$  with active carbon as reducing agent. Meanwhile, the influence of the dosage of citric acid and the amount of reducing agent on the magnetic properties of the samples was discussed. The structure, magnetic and electrical properties of the samples were investigated by various methods and the conductive mechanism of the sample was studied.

## Experimental

### *Synthesis of $\text{Sr}_2\text{FeMoO}_6$*

Polycrystalline  $\text{Sr}_2\text{FeMoO}_6$  samples were prepared by Sol-Gel method. Stoichiometric powders of  $\text{Sr}(\text{NO}_3)_2$ ,  $\text{Fe}(\text{NO}_3)_3 \cdot 9\text{H}_2\text{O}$  and  $(\text{NH}_4)_6\text{Mo}_7\text{O}_{24} \cdot 4\text{H}_2\text{O}$  were mixed with citric acid and then dissolved with distilled water. The pH of the solution was adjusted to 3 by aqueous ammonia in concentration of 5 mol/L under consecutively stirring. A slight green gel was formed after several hours under the condition of water bath at 60 °C. Then the gel was put into oven and pyrolyzed for 3 h at 180 °C. The dry gel was frothed, fumed and finally formed a dry black sponge (which was called precursor). Then the precursor was pre-sintered for 5 h at 600 °C. Finally, the powder was mixed with appropriate active carbon powder and then sintered for 3 h at 1200 °C in the reducing atmosphere provided by active carbon particles to obtain the final product.

### *Characterization*

The crystal structure and the phase purity of the samples were investigated by x-ray powder diffraction (XRD) using a Y2000 diffractometer with Cu  $K\alpha$  radiation (30kV×20mA) at room temperature. XRD was performed on powdered samples over the  $2\theta$  range of 15° to 75°. A step scan mode was employed with a step width of  $2\theta = 0.06^\circ$  and a sampling time of 1s. The size and morphology of the samples were observed with a KYKY-2800B scanning electron microscope (SEM). The temperature dependence of the zero-field-cooled magnetization (M-T) was obtained with a vibrating sample magnetometer (VSM) in the temperature range of 80-300 K and the magnetic field of 0.5 T. The same equipment was used to measure the M-H loop at room temperature. Transport properties were determined by a standard four-probe DC method in the temperature range 80~300 K.

## Results and Discussion

### *Effect of the dosage of citric acid and the reductant on magnetic properties and phase structure*

Citric acid (CA) is an organic ternary acid. It can form stable complexes with most of metal ions due to the tridentate ligand nature and three-dimensional network upon gel can be formed

by the condensation reaction of CA, which can greatly inhibit metal ions segregation and/or fluctuation of chemical constituents. Therefore, appropriate amount of citric acid is conducive to the formation of stable sol - gel system.

In consideration of activated carbon as the solid reductant, the residual carbon from the pyrolysis of the complex will affect the dosage of activated carbon and the properties of the sample. So the amount of citric acid needs to be considered with the amount of activated carbon.

In this paper, active carbon is used for reducing agent and the reducing atmosphere is provided by active carbon particles outside the small crucible. Under high temperature,  $\text{Mo}^{6+}$  is reduced by active carbon and turns into  $\text{Mo}^{5+}$  (some  $\text{Fe}^{3+}$  may be reduced into  $\text{Fe}^{2+}$ ) and the active carbon is oxidized into CO.

According to charge conservation law, the molar ratio of active carbon to sample is 0.5:1. But the actual dosage of reductant active carbon is higher than the theoretical value considering the influence of external oxidizing substance.

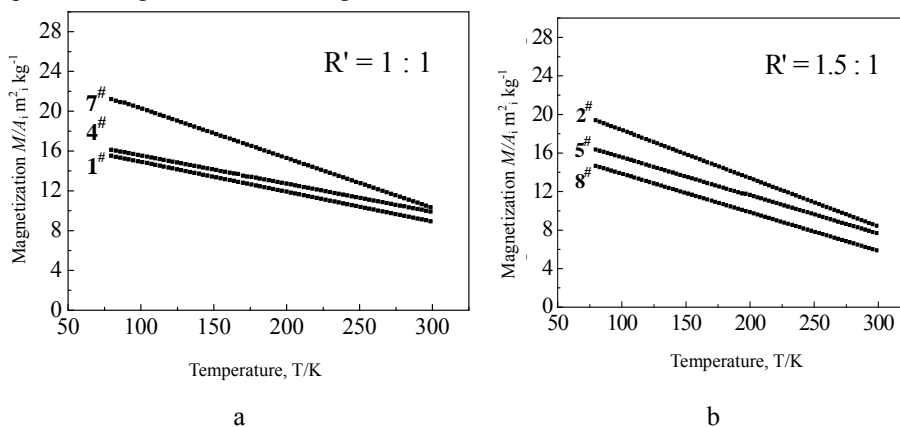
A series of experiments (Table 1) is designed to define the dosages of citric acid and active carbon. The molar ratio (R) of CA and metal ions were changed from 1:1, 1.5:1 to 2:1 and the molar ratio (R') of active carbon to the pre-sintering product is 1:1, 1.5:1 and 2:1 respectively in these experiments.

**Table 1.** Optimization of the dosages of citric acid and active carbon

	R' = 1 : 1	R' = 1.5 : 1	R' = 2 : 1
R = 1 : 1	1 <sup>#</sup>	2 <sup>#</sup>	3 <sup>#</sup>
R = 1.5 : 1	4 <sup>#</sup>	5 <sup>#</sup>	6 <sup>#</sup>
R = 2 : 1	7 <sup>#</sup>	8 <sup>#</sup>	9 <sup>#</sup>

1<sup>#</sup>~9<sup>#</sup>: Number of samples

Figure 1 (a), (b) and (c) show the curves of the magnetization versus temperature (M-T) of samples under constant R' and different R. It can be seen from Figure 1 (a) that the magnetization increases with the increase of the dosage of citric acid when the dosage of active carbon is fewer. While Figure 1(b) and (c) show that the magnetization decreases with the increase of the dosage of citric acid when the dosage of active carbon is larger. Figure 1(a), (b) and (c) also shows that the magnetization of sample at room temperature decreases obviously with increasing the dosage of active carbon. Among them, the magnetization of 7<sup>#</sup> sample is the highest under the magnetic field of 0.5 T.



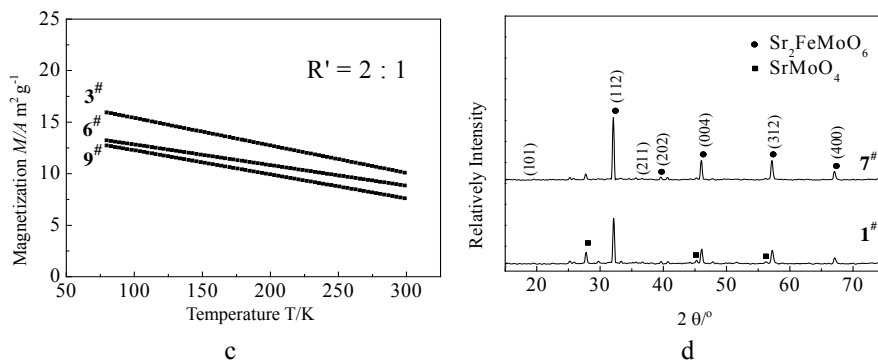


**Figure 1.** Influence of the dosage of citric acid and active carbon on magnetism and phase structure

In order to investigate the effect of citric acid dosage on the phase structure, XRD patterns of 1<sup>#</sup> and 7<sup>#</sup> sample were measured and shown in Figure 1 (d). According to that, main phase of the samples are crystalline double Perovskite  $\text{Sr}_2\text{FeMoO}_6$ . Based on the space group I4/mmm, the reflections can be indexed by the Jade5 program and unit cell parameter is  $a = 5.580\text{\AA}$ ,  $c = 7.882\text{\AA}$ . The appearance of the superstructure reflection peaks of (101) and (211) indicates part of  $\text{Fe}^{3+}$  and  $\text{Mo}^{5+}$  ions orderly occupy on B and B' sites, respectively. Moreover, it is found that there are fewer impurity phase ( $\text{SrMoO}_4$ , JCPDS No. 08-0482) in 7<sup>#</sup> sample than that in 1<sup>#</sup> and the intensity of diffraction peaks of  $\text{Sr}_2\text{FeMoO}_6$  in 7<sup>#</sup> sample are stronger than those in 1<sup>#</sup>.

Therefore, in order to obtain pure phase and better magnetic properties, the molar ratio of citric acid to metal ions is determined to 2:1 and that of active carbon to pre-sintering product is 1:1 (7<sup>#</sup> sample).

Based on the M-T curve of sample 7<sup>#</sup> in Figure 1 (a), the reduction rate of the magnetization versus temperature is only  $0.078 \text{ A}\cdot\text{m}^2/\text{kg}\cdot\text{K}$  in the range of 80~300 K, which indicates that the magnetization decreases slowly with increasing temperature and the magnetic structure has not been changed in this temperature range. This shows that the Curie temperature of the sample is higher than 300 K.

The M-H curve of sample 7<sup>#</sup> in Figure 2 shows that the magnetization is still not saturated as the applied field rises to 1.0 T from 0.0 T. The saturation magnetization of this sample is  $13.321 \text{ A}\cdot\text{m}^2/\text{kg}$ , which is obtained as the linear part of magnetization versus  $1/H$  curve was extrapolated to  $1/H = 0$ .

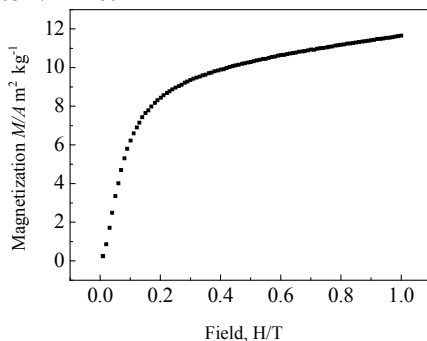


**Figure 2.** M-H curve of  $\text{Sr}_2\text{FeMoO}_6$

### Electrical transport properties

Figure 3 shows temperature dependence of resistivity. The resistivity exhibits typical semiconductor behavior ( $d\rho/dT < 0$ ) in temperature range from 80 to 300 K, which are measured under 0.0 T and 1.0 T, respectively. Figure 4 shows that the relationship of  $\ln(\rho/T)$  with  $1/T^{1/4}$  is very satisfactorily linear ( $r = 0.9995$ ), which is fitted with small polaron variable range hopping model<sup>12</sup>.

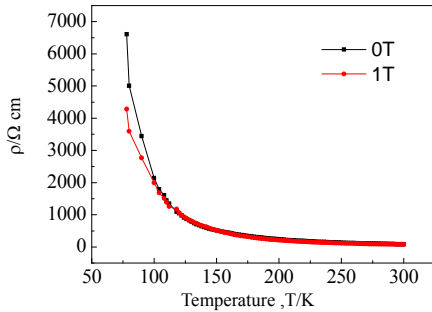


**Figure 3.**  $\rho$ -T curves of  $\text{Sr}_2\text{FeMoO}_6$

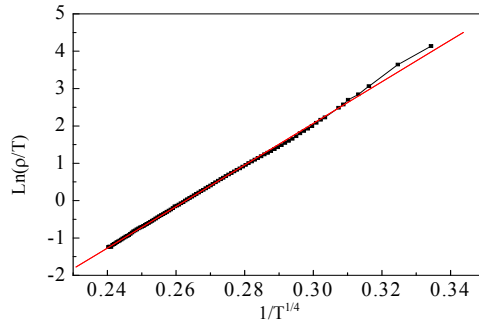


**Figure 4.**  $\ln(\rho/T) \sim 1/T^{1/4}$  pattern of  $\text{Sr}_2\text{FeMoO}_6$

MR is determined using the formula:

$$MR = \frac{\rho(H) - \rho(0)}{\rho(0)} \times 100\%$$

Where  $\rho(0)$  and  $\rho(H)$  are resistivity in zero and applied field, respectively. Figure 5 shows the temperature dependence of MR ratio of  $\text{Sr}_2\text{FeMoO}_6$  under 1.0 T field. It can be seen that the MR ratio of the sample is nearly -7% ~ -10% at a low magnetic field of 1.0 T over a temperature range from 170 to 300 K. MR ratio is recorded to be -10.02% at 300 K, which shows significant negative magnetoresistance at room temperature and is higher than the values of the samples obtained by traditional solid state reaction reported in literature<sup>7,13,14</sup>, even higher than the early report of sol-gel routine<sup>11</sup>.

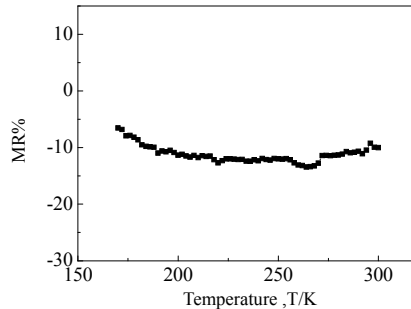


**Figure 5.** Temperature dependence of MR ratio of  $\text{Sr}_2\text{FeMoO}_6$

### Micromorphology analysis

Figure 6 is the SEM photograph of  $\text{Sr}_2\text{FeMoO}_6$  obtained under the above appropriate conditions. It can be seen from Figure 6 that the initial particles are nearly spherical in shape and very small with diameter below 100 nm. While the grain size of the samples obtained by traditional solid state reaction are always micron-grade<sup>14</sup>. Smaller grain size leads to larger grain boundaries, which leads to larger MR effect at low applied field. Meanwhile, some big particles with irregular shape can be observed, which may result from large surface energy of the initial small particles during the post calcination process.

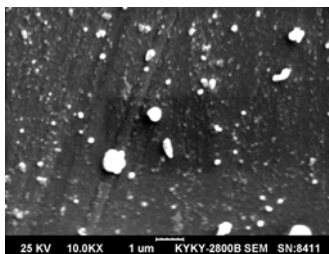


**Figure 6.** SEM photograph of the  $\text{Sr}_2\text{FeMoO}_6$  sample

## Conclusion

- The double Perovskite oxide  $\text{Sr}_2\text{FeMoO}_6$  was prepared successfully by sol-gel method using activated carbon as reducing agent. This method has the advantages of uniformity of product ingredients, small particle size, easy operation, and so on.
- The as-synthesized sample has relatively pure phase and excellent magnetic properties when the ratio of citric acid and metallic ions in mole is 2:1, the mole ratio of active carbon powder and pre-sintering product is 1:1.
- The as-synthesized sample exhibits typical semiconductor behavior with small polaron variable range hopping conductive mechanism and significant negative magnetoresistance.

## Acknowledgment

This study was supported by National Natural Science Foundation of China (China, No. 50672020). We gratefully acknowledge their support during the study.

## References

1. Daughton J M, *J Magn Magn Mater.*, 1999, **192(2)**, 334-342.
2. Prinz G A, *Science*, 1999, **282(5394)**, 1660-1663.
3. Jin S, Tiefel T H, McCormack M, Fastnacht R A, Ramesh R and Chen L H, *Science*, 1994, **264(5157)**, 413-415.
4. Xiong G C, Li Q, Ju H L, Mao S N, Senapati L, Xi X X, Greene R L and Venkatesan T, *Appl Phys Lett.*, 1995, **66(11)**, 1427-1429.
5. Bonaedy T, Song K M, Sung K D, Hur N and Jung J H, *Solid State Commun.*, 2008, **148(9-10)**, 424-427.
6. Zener C, *Phys Rev.*, 1951, **82(3)**, 403-405.
7. Kobayashi K I, Kimura T, Sawada H, Terakura K and Tokura Y, *Nature*, 1998, **395(15)**, 677-680.
8. Sarma D D, Mahadevan P, Saha-Dasgupta T, Ray S and Kumar A, *Phys Rev Lett.*, 2000, **85(12)**, 2549-2552.
9. Kobayashi K I, Kimura T, Tomioka Y, Sawada H, Terakura K and Tokura Y, *Phys Rev B*, 1999, **59(17)**, 11 159.
10. Zhang Q, Rao G H, Xiao Y G, Dong H Z, Liu G Y, Zhang Y and Liang J K, *Physica B: Condens Matter*, 2006, **381(1-2)**, 233-238.
11. Yuan C L, Wang S G, Song W H, Yu T, Dai J M, Ye S L and Sun Y P, *Appl Phys Lett.*, 1999, **75(24)**, 3853-3855.
12. Jaime M, Salamon M B, Pettit K, Rubinstein M, Treece R E, Horwitz J S and Chrisey D B, *Appl Phys Lett.*, 1996, **68(11)**, 1576-1580.
13. Sarma D D, Sampathkumaran E V, Ray S, Nagarajan R, Majumdar S, Kumar A, Nalini G and Guru Row T N, *Solid State Commun.*, 2000, **114(9)**, 465-468.
14. Rao G N, Roy S, Mou C Y and Chen J W, *J Magn Magn Mater.*, 2006, **299(2)**, 348-355.



**Hindawi**

Submit your manuscripts at  
<http://www.hindawi.com>

